International Journal of Nanomedicine

Dovepress
Taylor & Francis Group

Open Access Full Text Article

ORIGINAL RESEARCH

Protective Effects of Orally Administered *Salvia miltiorrhiza*–Derived Extracellular Vesicles on Diabetic Kidney Disease: Protection Mediated by Gut Microbiota and Metabolomic Remodeling

Yi Liu[1,*], Zhiying Feng[1,*], Jiawang Huang[1], Jiacheng He[2], Liu Li[1], Rong Yu[1]

[1]College of Traditional Chinese Medicine of Hunan University of Chinese Medicine, Changsha, Hunan, 410208, People's Republic of China; [2]College of Integrated Traditional Chinese and Western Medicine of Hunan University of Chinese Medicine, Changsha, Hunan, 410208, People's Republic of China

*These authors contributed equally to this work

Correspondence: Rong Yu; Jiawang Huang, College of Traditional Chinese Medicine, Hunan University of Chinese Medicine, Xueshi Road 300, Changsha, Hunan, 410208, People's Republic of China, Email yurong196905@163.com; 1518522909@qq.com

Purpose: Diabetic kidney disease (DKD) is one of the most common and severe microvascular complications of diabetes, characterized by glomerulosclerosis and tubulointerstitial fibrosis. Growing evidence indicates that gut dysbiosis and metabolic imbalance contribute to DKD progression. *Salvia miltiorrhiza* possesses anti-inflammatory, antioxidative, and antifibrotic activities, while *Salvia miltiorrhiza*-derived Extracellular Vesicle (SMEVs), as natural nano-carriers, exhibit favorable bioactivity and targeting potential.

Methods: SMEVs were isolated and purified using differential centrifugation combined with sucrose density gradient ultracentrifugation. Transmission electron microscopy and nanoparticle tracking analysis confirmed their typical bilayer membrane and an average diameter of approximately 163.6 nm. BKS.DB mice were orally administered SMEVs for 6 weeks, followed by evaluation of renal function, histopathology, and molecular markers.

Results: SMEV treatment significantly improved glucose and lipid metabolism, reduced proteinuria, alleviated renal dysfunction, and mitigated renal fibrosis in DKD mice. 16S rRNA sequencing revealed that SMEVs reshaped the gut microbial community by increasing beneficial taxa and suppressing pathogenic bacteria. Untargeted metabolomics demonstrated that SMEVs reversed DKD-associated metabolic disturbances, characterized by the upregulation of bioactive peptides (eg, Tyr-Leu-His) and unsaturated fatty acids (eg, petroselinic acid), along with the reduction of pro-inflammatory lipids. KEGG enrichment indicated significant modulation of arachidonic acid, linoleic acid, and amino acid metabolism pathways. Spearman correlation analysis further revealed strong associations between key microbial taxa and differential metabolites, suggesting coordinated regulation of gut microbiota and metabolism during SMEV-mediated protection.

Conclusion: SMEVs significantly improve the pathological progression of DKD by reshaping the intestinal flora, restoring metabolic homeostasis and inhibiting inflammatory and fibrotic responses, providing an experimental basis for the application of plant-derived extracellular vesicles in kidney diseases.

Keywords: diabetic kidney disease, gut microbiota, *Salvia miltiorrhiza*–derived extracellular vesicles, extracellular vesicles, metabolomics

Introduction

Diabetes mellitus (DM) is a metabolic disorder characterized by chronic hyperglycemia and remains a major global public health challenge. According to the International Diabetes Federation, the number of individuals with DM reached 537 million worldwide in 2024 and is projected to increase to 783 million by 2045.[1] Diabetic kidney disease (DKD), one of the most common and severe microvascular complications of DM, develops in approximately 30–40% of diabetic patients and has become the leading cause of end-stage renal disease (ESRD). Its incidence continues to rise, imposing a substantial public health burden.[2] Currently available therapies for DKD mainly rely on glycemic and blood pressure

https://doi.org/10.2147/IJN.S580968
Received: 26 November 2025
Accepted: 1 February 2026
Published: 13 February 2026

control, as well as renin–angiotensin system inhibitors. However, these treatments primarily target metabolic or hemodynamic abnormalities and are insufficient to fully block inflammatory and oxidative injury pathways. Moreover, concerns regarding long-term side effects and safety profiles remain.[3] Therefore, the development of natural agents with both safety advantages and multi-target regulatory properties has become an emerging research focus.

The gut microbiota is an integral component of the host and plays a crucial role in maintaining metabolic homeostasis. Alterations in its composition and metabolic activity can lead to dysbiosis, which disrupts normal metabolic processes and has been strongly linked to diabetes and other metabolic diseases.[4] Gut microbiota dysbiosis contributes to the onset and progression of DKD through mechanisms involving hemodynamic alterations, impaired glucose and lipid metabolism, and changes in microbial-derived metabolites.[5] According to the gut–kidney axis theory, interactions among impaired intestinal barrier function, disrupted gut microbiota, and reduced glomerular filtration rate highlight the close connection between the intestine and kidney in metabolic regulation, immune–inflammatory responses, and the structural and functional integrity of the gut mucosa and microbiota.[6] Increasing evidence indicates that DKD is driven by multiple factors. Beyond hyperglycemia-induced oxidative stress and inflammation, shifts in microbial metabolites can reach the kidney via the circulatory system and disturb renal metabolic homeostasis, underscoring the critical role of the gut–kidney axis in DKD progression.[6] In DM and its complications, gut microbial diversity is significantly reduced, characterized by a decline in short-chain fatty acid (SCFA)-producing bacteria and an increase in endotoxin-producing taxa such as Enterobacteriaceae.[7] Dysbiosis can influence DKD through several pathways: reduced SCFA-producing probiotics impair intestinal barrier integrity and promote endotoxemia; alterations in taxa involved in tryptophan and bile acid metabolism disrupt renal immune regulation; and expansion of uremic toxin–producing bacteria enhances tubular toxicity.[8] Therefore, modulation of gut microbiota and microbial metabolites has emerged as a promising therapeutic strategy for preventing and managing DKD.

Salvia miltiorrhiza Bunge (commonly known as danshen) is a traditional Chinese medicinal herb with multiple pharmacological activities, including antioxidant, anti-inflammatory, antifibrotic, and endothelial-protective effects. Its major bioactive constituents consist of lipophilic diterpenoid quinones and hydrophilic phenolic acids.[9,10] Compounds such as tanshinone I, tanshinone IIA, and cryptotanshinone exhibit marked anti-inflammatory, antioxidant, and anti-apoptotic activities, whereas salvianolic acid A and salvianolic acid B exert free radical–scavenging effects and inhibit the release of inflammatory mediators.[11] Tanshinone IIA has been reported to delay DKD progression by regulating the Txnip/NLRP3 inflammasome pathway and inhibiting pyroptosis.[12] However, the clinical application of *Salvia miltiorrhiza* remains limited by the poor solubility, low oral bioavailability, rapid metabolism, and weak tissue selectivity of its major active constituents. Moreover, traditional Danshen extracts contain multiple bioactive constituents without a defined delivery structure, which complicates the systematic investigation of their integrated mechanisms of action and limits precise attribution at the pathway or organ level.[13,14]

In recent years, extracellular vesicles (EVs) have attracted increasing attention as important mediators of intercellular communication due to their favorable biocompatibility and capacity for cross-species signal transfer.[15] Plant-derived extracellular vesicles (PDEVs) are nanoscale vesicles actively secreted by plant cells and are enriched in bioactive components, including lipids, proteins, and nucleic acids. These vesicles are capable of mediating inter-kingdom communication and modulating host physiological functions.[16] Accumulating evidence indicates that EVs derived from medicinal plants, such as Platycodon grandiflorus and Citrus reticulata, exhibit anti-inflammatory, antioxidant, and immunomodulatory properties, thereby ameliorating inflammatory disorders and metabolic dysfunctions.[17,18] Compared with conventional herbal extracts, traditional Chinese medicine–derived EVs can encapsulate lipophilic or chemically unstable bioactive compounds, thereby improving their stability and bioavailability, and potentially enabling targeted delivery and synergistic therapeutic effects.[19,20] However, investigations into the role of PDEVs in renal diseases remain limited, and systematic mechanistic studies focusing on the gut–kidney axis are particularly scarce. PDEVs possess an intrinsic resistance to the harsh gastrointestinal environment, including acidic pH and digestive enzymes, which is largely attributed to their phospholipid-rich bilayer structure and abundant bioactive cargos. Previous studies have demonstrated that orally administered PDEVs extracted from medicinal plants can be detected within the gastrointestinal tract and preferentially accumulate in the intestine, where they exert biological effects through interactions with intestinal epithelial cells and the gut microbiota.[21,22] On this basis, extracellular vesicles derived from *Salvia miltiorrhiza*

(SMEVs) may represent a novel delivery system capable of overcoming the limitations of conventional *Salvia miltiorrhiza* formulations. In the present study, SMEVs were extracted, purified, and characterized, and their protective effects against DKD, as well as the underlying mechanisms, were systematically investigated. The structural features of SMEVs were confirmed through morphological and physicochemical analyses. Furthermore, in vivo experiments combined with 16S rRNA gene sequencing and untargeted metabolomic profiling were employed to elucidate the role of SMEVs in modulating the gut–kidney axis. This study aims to provide new mechanistic insights and theoretical support for the development of SMEVs as a potential oral therapeutic strategy for the prevention and treatment of DKD.

Materials and Methods

Experimental Reagents and Instruments

Experimental Reagents

Dapagliflozin tablets (AstraZeneca Pharmaceuticals LP, HJ20170119) were obtained from the First Affiliated Hospital of Hunan University of Chinese Medicine. The bicinchoninic acid (BCA) protein assay kit (Lianke Bio, 81910335A), 4% paraformaldehyde solution (Solarbio, P1117), Masson's trichrome staining kit (Solarbio, G1340), 5% bovine serum albumin (BSA) blocking solution (Solarbio, SW3015), hematoxylin–eosin (H&E) staining kit (Solarbio, G1120), DAB chromogenic kit (Solarbio, DA1010), horseradish peroxidase (HRP)-conjugated antibody diluent (Solarbio, A1820), and phosphate-buffered saline (PBS; Solarbio, P1020) were purchased from Beijing Solarbio Science&Technology Co., Ltd. The near-infrared fluorescent dye 1,1′-dioctadecyl-3,3,3′,3′-tetramethylindotricarbocyanine iodide (DiR; Thermo Fisher Scientific, D12731) was obtained from Thermo Fisher Scientific. Urinary protein quantification kits (Nanjing Jiancheng Bioengineering Institute, C035-2-1), creatinine (CRE) assay kits (C011-2-1), blood urea nitrogen (BUN) assay kits (C013-2-1), uric acid (UA) assay kits (C012-1-1), and triglyceride (TG) assay kits (A110-2-1) were purchased from Nanjing Jiancheng Bioengineering Institute. Xylene (Sinopharm Chemical Reagent,10023418), absolute ethanol (Sinopharm Chemical Reagent,10009218), and citrate buffer (Sinopharm Chemical Reagent,72015060) were obtained from Sinopharm Chemical Reagent Co., Ltd. Theα-smooth muscle actin (α-SMA) rabbit monoclonal antibody (ABclonal, A2235; 1:200) was purchased from ABclonal Biotechnology Co., Ltd. Isoflurane anesthetic (RWD Life Science, R510-22-10) was supplied by the Animal Experimental Center of Hunan University of Chinese Medicine.

Experimental Instruments

A benchtop high-speed refrigerated centrifuge (Thermo Fisher Scientific), a quantitative real-time PCR system (Bio-Rad) , an Optima MAX-XP tabletop ultracentrifuge (Beckman Coulter), a nanoparticle tracking analysis system (NanoSight, Malvern), a CO_2 cell culture incubator (Thermo Fisher Scientific), an inverted microscope (Motic), an upright fluorescence microscope (Nikon), a Synergy 2 multimode microplate reader (BioTek), a transmission electron microscope (Hitachi), precision micropipettes (High Tech Lab), an ultramicrovolume spectrophotometer (Bio-Rad, USA), a pathological tissue slicer (Leica), a light microscope (Olympus, Japan), a constant-temperature slide dryer (Leica, Germany), a paraffin microtome (Leica, Germany), and an IVIS Lumina Series III in vivo optical imaging system for small animals (PerkinElmer, USA) were used in this study.

Experimental Animals

Male DB/M and BKS.DB mice (8 weeks old, 18–22g) were purchased from Hangzhou Ziyuan Laboratory Animal Technology Co., Ltd. (license 20250529Abbz01050000009). All animals were housed at the Animal Experimental Center of Hunan University of Chinese Medicine. All animal procedures were conducted in accordance with the guidelines of the American Veterinary Medical Association (AVMA) Guidelines for the Euthanasia of Animals (2020 Edition) and the national regulations on the administration of laboratory animals. The study protocol was reviewed and approved by the Institutional Animal Care and Use Committee of Hunan University of Chinese Medicine (Approval 202510025). Mice were maintained under standard environmental conditions (temperature 22 °C, humidity 50±5%) with a 12-h light/dark cycle. BKS.DB mice were randomly assigned to the model group (Model, n=6), positive control group (Dap, n=6), and SMEV-treated group (SMEV, n=6). Age-matched DB/M mice served as the normal control group (Control). Mice in the SMEV group received SMEVs by oral gavage at 25 mg/kg/day; mice in the positive control group

received dapagliflozin at 2.05 mg/kg/day; and mice in the model and control groups received equal volumes of saline. After 6 weeks of oral treatment, mice were anesthetized with inhaled isoflurane (induction at 3–4%, maintenance at 1.5–2% in oxygen) prior to blood collection to ensure adequate anesthesia and to minimize pain and distress. At the end of the experiment, animals were euthanized under deep anesthesia using cervical dislocation, a method consistent with AVMA-approved physical euthanasia techniques for small laboratory rodents. All efforts were made to minimize animal suffering, reduce the number of animals used, and ensure humane endpoints. Mice were anesthetized with isoflurane, blood samples were collected immediately, and kidney tissues and intestinal contents were harvested for further analyses.

Isolation, Purification, and Characterization of SMEVs

Isolation and Purification of SMEVs

Fresh *Salvia miltiorrhiza* juice was subjected to differential centrifugation at 4 °C (2000×g for 20 min and 10,000×g for 60 min). The supernatant was collected, filtered through a 0.45 μm membrane, and ultracentrifuged at 150,000×g for 90 min at 4 °C. The pellet was resuspended in PBS and further purified by sucrose density gradient ultracentrifugation (8%, 30%, 45%, and 60%) at 150,000×g for 90 min. The interphase fractions between 8–30% and 30–45% sucrose layers were collected, washed with PBS, and resuspended to obtain purified SMEVs.

Morphological Observation of SMEVs by Transmission Electron Microscopy (TEM)

A drop of SMEV suspension was placed onto a copper grid and allowed to stand for 3–5 min. The sample was stained with 3 % phosphotungstic acid for 5 min, air-dried, and imaged under a transmission electron microscope.

Nanoparticle Tracking Analysis (NTA)

SMEV pellets were resuspended in PBS, mixed thoroughly, and analyzed at room temperature using a nanoparticle tracking analyzer to determine particle size distribution.

Protein quantification of SMEVs by bicinchoninic acid (BCA) assay

Standard solutions and BCA working reagent were prepared according to the manufacturer's protocol. A total of 200 μL BCA working reagent and 20 μL standard or SMEV sample were added to each well of a 96-well plate and incubated at 37 °C for 30 min in the dark. Protein concentrations were measured using a microplate reader.

Ex vivo Biodistribution of Orally Administered SMEVs

BKS.DB mice were orally administered DiR fluorescent dye–labeled SMEVs at a dose of 25 mg/kg. Mice were anesthetized with isoflurane and humanely euthanized by cervical dislocation performed by trained personnel. Subsequently, the small intestine, colon, liver, kidneys, spleen, lungs, and heart were harvested, and ex vivo fluorescence imaging was performed using an IVIS Lumina imaging system to assess the organ-specific distribution of DiR fluorescence signals.

Measurement of Biochemical Parameters

Twenty-four-hour urine samples were collected from mice in each group using metabolic cages. Urinary albumin and urinary creatinine levels were measured using commercial assay kits (Nanjing Jiancheng Bioengineering Institute, China), and the urine albumin-to-creatinine ratio (UACR) as well as 24-hour urinary protein excretion were calculated to assess the severity of proteinuria. During the experimental period, body weight and fasting blood glucose levels were monitored weekly. At the end of the experiment, blood samples were collected and centrifuged at 3000×g for 15 min to obtain serum. Serum blood urea nitrogen (BUN), creatinine (CREA), uric acid (UA), and triglyceride (TG) levels were determined using commercial assay kits (Nanjing Jiancheng Bioengineering Institute, China) according to the manufacturers'instructions. All measurements were performed in strict accordance with the corresponding protocols provided by the manufacturers.

Histological Staining

Kidney tissues were fixed in 4% paraformaldehyde overnight, dehydrated, embedded in paraffin, and sectioned into 3–4 μm slices. (1) Hematoxylin–eosin (HE) staining: Sections were dewaxed with xylene and rehydrated through graded

ethanol. Hematoxylin staining, differentiation, bluing, and eosin staining were performed sequentially, followed by ethanol dehydration, xylene clearing, and mounting. HE staining was used to assess overall glomerular and tubular morphology. (2) Masson's trichrome staining: After dewaxing and rehydration, sections were stained according to the manufacturer's instructions, including nuclear staining, cytoplasmic staining, and collagen fiber staining. Sections were dehydrated, cleared, and mounted. Masson staining was used to evaluate collagen deposition in the renal interstitium. (3) Immunohistochemistry (IHC): Dewaxed and rehydrated sections underwent antigen retrieval using citrate buffer (pH 6.0) in a heat-induced retrieval system. After cooling, endogenous peroxidase activity was blocked with 3% H_2O_2, followed by 5% BSA blocking for 30 min. Sections were incubated with primary antibodies at 4 °C overnight. After PBS washing, HRP-conjugated secondary antibodies were applied, followed by DAB chromogenic development and hematoxylin counterstaining. Sections were then dehydrated, cleared, mounted, and imaged under an optical microscope.

16S rRNA Sequencing and Data Analysis

Genomic DNA from intestinal content samples was extracted using the CTAB/SDS method. DNA purity and concentration were assessed by agarose gel electrophoresis, and samples were diluted to 1 ng/μL. Diluted DNA was used as the template for PCR amplification with barcoded specific primers (eg, 16S V4 region: 515F/806R) and Phusion® High-Fidelity PCR Master Mix. PCR products were examined by agarose gel electrophoresis, purified with magnetic beads, quantified, and pooled in equimolar amounts, followed by gel recovery using the Qiagen Gel Extraction Kit. Sequencing libraries were constructed using the TruSeq® DNA PCR-Free Sample Preparation Kit. After quantification by Qubit and qPCR, sequencing was performed on the Illumina NovaSeq 6000 platform with paired-end reads. Raw reads were demultiplexed based on barcodes and processed using fastp for quality filtering and adapter trimming. High-quality tags were generated using FLASH, and chimeric sequences were removed using vsearch to obtain effective tags. Operational taxonomic units (OTUs) were clustered at 97% similarity using the Uparse algorithm in USEARCH v7, while amplicon sequence variants (ASVs) were generated using QIIME 2/Deblur for denoising. OTU/ASV taxonomic annotation was performed with Mothur against the SILVA SSU rRNA database (threshold 0.8–1). Phylogenetic trees were constructed using MAFFT. All samples were rarefied to the same sequencing depth. Alpha diversity indices (Chao1, Shannon, Simpson, etc), rarefaction curves, and rank abundance curves were calculated and visualized using R packages phyloseq and vegan. Beta diversity was calculated based on UniFrac distances and visualized by principal component analysis (PCA), principal coordinates analysis (PCoA), and non-metric multidimensional scaling (NMDS). Statistical analyses included *t*-test, Wilcoxon test, Tukey's test, and Kruskal–Wallis test. Differential taxa were identified using LEfSe (LDA>4). Community structural differences were evaluated using Anosim, MRPP, Adonis, and AMOVA.

Metabolomics Analysis of Intestinal Contents

Raw LC–MS data were subjected to peak detection, filtering, and alignment to generate a quantitative dataset of detected metabolites, and a base peak chromatogram was constructed. Metabolite identification was performed by matching against public databases including HMDB, MassBank, LipidMaps, mzCloud, and KEGG, as well as an in-house library. Data correction was applied to eliminate systematic errors. During quality control, metabolites with relative standard deviation (RSD)>30% in QC samples were excluded. The processed dataset was scaled and subjected to hierarchical clustering for both samples and metabolites using the R package pheatmap. After data normalization, multivariate statistical analyses were conducted, including PCA, partial least squares–discriminant analysis (PLS-DA), and orthogonal PLS-DA (OPLS-DA). For pairwise comparisons, differential metabolites were screened based on VIP>1 and $P<0.05$ (Student's *t*-test). For multiple-group comparisons, metabolites with VIP>1 and $P<0.05$ (ANOVA) were selected. VIP values were extracted from the OPLS-DA model, which also included score plots and permutation tests (200 permutations) to prevent overfitting, implemented using the R package MetaboAnalystR. Prior to OPLS-DA, data were $\log_2$-transformed and mean-centered. Identified metabolites were annotated using the KEGG Compound database and mapped to the KEGG Pathway database. Significantly enriched pathways were identified by hypergeometric testing with false discovery rate (FDR) correction, and FDR<0.05 was set as the threshold. Pathway enrichment analysis was carried out using the R package clusterProfiler, and results were visualized as bubble plots in which bubble size indicates metabolite count and bubble color represents enrichment significance.

Statistical Analysis

All data were expressed as mean±standard deviation ($\overline{x} \pm s$). Normality was assessed using the Shapiro–Wilk test, and homogeneity of variance was evaluated with Levene's test. For data with normal distribution and equal variance, group comparisons were conducted using one-way ANOVA followed by Tukey's post hoc test. For non-normally distributed data, the Kruskal–Wallis test was applied. A P value<0.05 was considered statistically significant. Graphs were generated using GraphPad Prism. Spearman correlation analysis was used to evaluate associations among differential gut microbial taxa, differential metabolites, and renal function parameters. All statistical tests were two-sided, and P<0.05 was considered statistically significant.

Results

Isolation, Purification, and Characterization of SMEVs

SMEVs were isolated and purified using differential centrifugation combined with sucrose density gradient ultracentrifugation (Figure 1A). Transmission electron microscopy revealed that SMEVs exhibited a typical round or oval morphology with a bilayer membrane structure (Figure 1B). Protein electrophoresis analysis confirmed the presence of protein components within SMEVs (Figure 1C). The NTA results demonstrated a homogeneous size distribution, with an average size of 163.6 nm (Figure 1D). The protein concentration of SMEVs, as determined by the BCA assay, was 6.03 mg/mL, indicating a high protein content in SMEVs (Figure 1E). Ex vivo biodistribution analysis of DiR-labeled SMEVs showed a pronounced fluorescence signal in the intestinal region (Figure 1F), indicating that orally administered SMEVs were preferentially retained in the gastrointestinal tract of mice.

Effects of SMEVs on Glucose and Lipid Metabolism in DKD Mice

Body weight, fasting blood glucose, and serum TG levels were measured in mice from each group. As the disease progressed, mice in the model group exhibited increased body weight (Figure 2A) and elevated fasting blood glucose levels (Figure 2B), accompanied by a concomitant increase in serum TG levels (Figure 2C). Treatment with SMEVs attenuated the increase in body weight and fasting blood glucose in DKD mice. After 6 weeks of treatment, serum TG levels were reduced in the SMEVs-treated group. These results indicate that SMEVs administration partially normalized body weight, blood glucose, and TG levels, suggesting an improvement in glucose and lipid metabolic disturbances in DKD mice.

Effects of SMEVs on Renal Function in DKD Mice

24-hour urinary protein excretion, Urinary ACR, serum CREA, BUN, and UA levels were assessed to evaluate renal function. Compared with the control group, mice in the model group exhibited significantly increased 24-hour urinary protein excretion (Figure 2D), urinary ACR (Figure 2E), serum CREA (Figure 2F), BUN (Figure 2G), and UA (Figure 2H), indicating the development of pronounced proteinuria and renal functional impairment. Following SMEVs treatment, all these parameters were significantly reduced relative to the model group, suggesting that SMEVs administration ameliorated proteinuria and improved renal functional indices in DKD mice.

Effects of SMEVs on Renal Histopathological Injury and Fibrosis in DKD Mice

To further evaluate the protective effects of SMEVs on renal structural integrity in DKD mice, kidney tissues from each group were subjected to HE and Masson's trichrome staining. HE staining revealed that kidneys from the control group exhibited intact and well-organized glomerular and tubular structures. In contrast, the model group displayed marked glomerular hypertrophy, mesangial expansion, tubular epithelial cell swelling and necrosis, as well as inflammatory cell infiltration, indicating pronounced renal tissue injury and inflammatory responses. Following SMEVs treatment, renal histological abnormalities were significantly attenuated, with improved glomerular morphology, relatively preserved tubular architecture, and reduced interstitial inflammation (Figure 3A). Masson's trichrome staining showed minimal collagen deposition in the control group, mainly localized to the vascular pole of glomeruli and the tubular interstitium. In the model group, extensive collagen accumulation was observed within the renal interstitium, indicative of significant renal fibrosis. SMEVs treatment

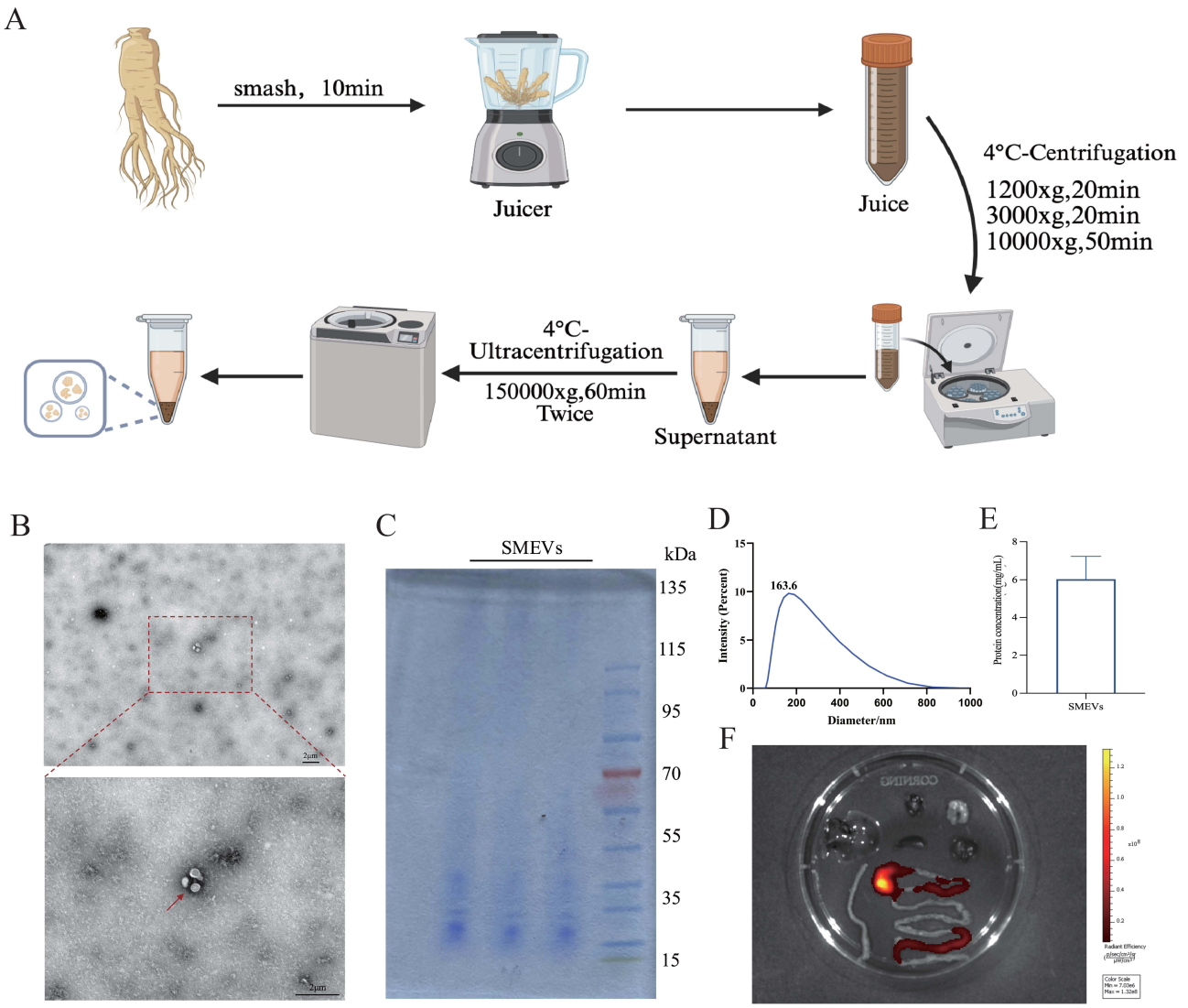

Figure 1 Isolation, purification, and characterization of SMEVs. (**A**) Schematic illustration of the isolation and purification procedure for SMEVs from *Salvia miltiorrhiza*. (**B**) Representative TEM image showing the typical bilayer membrane morphology of SMEVs. Scale bar=2 μm. Red arrows indicate representative SMEVs. (**C**) SDS-PAGE profile demonstrating the protein composition of SMEVs. (**D**) Size distribution of SMEVs determined by NTA. (**E**) Protein concentration of SMEVs quantified by the BCA assay. (**F**) Ex vivo biodistribution of DiR-labeled SMEVs after oral administration.

reduced collagen deposition, as evidenced by a decreased fibrotic area and lighter staining intensity, accompanied by partial restoration of renal tissue architecture (Figure 3B and D). Immunohistochemical analysis of α-smooth muscle actin (α-SMA) expression further demonstrated that α-SMA levels were increased in the tubulointerstitial region of the model group, reflecting active fibrogenesis. In contrast, SMEVs treatment significantly reduced α-SMA–positive staining intensity, and quantitative analysis confirmed a decreased α-SMA–positive area compared with the model group (Figure 3C and E). Collectively, these histological findings indicate that SMEVs administration ameliorated renal structural abnormalities and attenuated fibrosis-associated pathological changes in DKD mice.

Effects of SMEVs on Gut Microbiota in DKD Mice

To investigate the regulatory effects of SMEVs on gut microbiota composition in DKD mice, intestinal content samples from each group were subjected to 16S rRNA gene sequencing analysis. Distinct differences in microbial composition were observed among groups at the phylum, family, and genus levels. At the phylum level, the model group exhibited significantly increased relative abundances of Proteobacteria and Desulfobacterota, as well as an elevated Firmicutes/

https://doi.org/10.2147/IJN.S580968

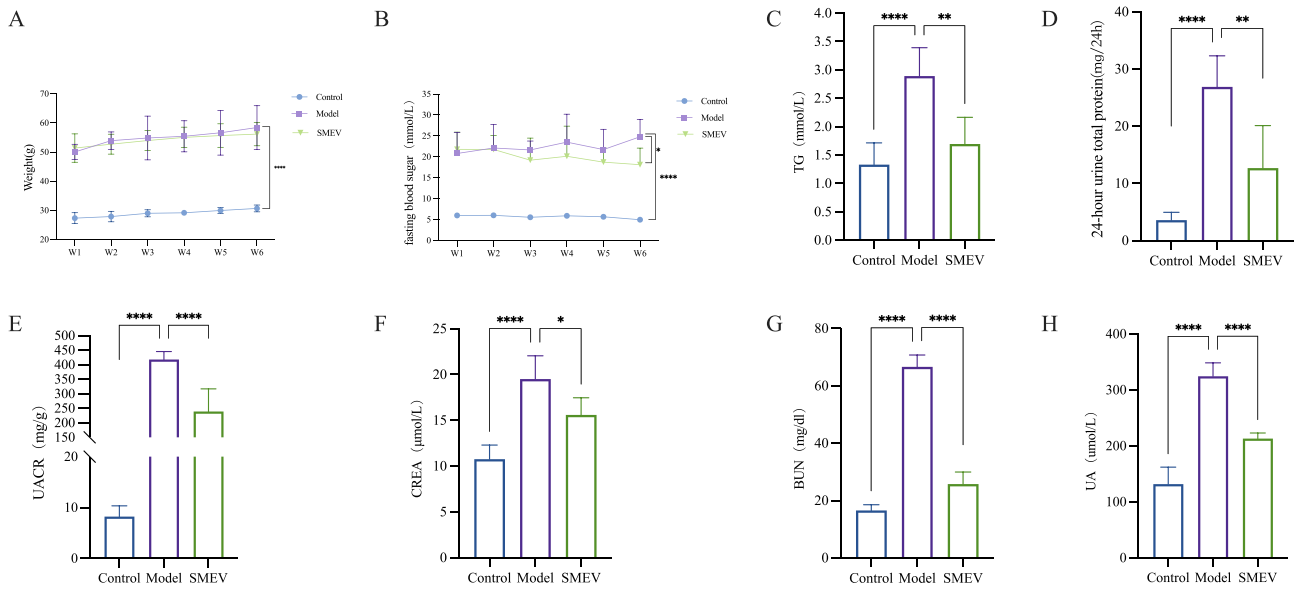

Figure 2 Effects of SMEVs on glucose and lipid metabolism, proteinuria, and renal function in mice with DKD. (**A**) Body weight. (**B**) Fasting blood glucose levels. (**C**) TG. (**D**) 24-hour urine total protein. (**E**) UACR. (**F**) CREA. (**G**) BUN. (**H**) UA. Data are presented as mean±SD (n=6 mice per group). *p<0.05, **p<0.01, ***p<0.001, ****p<0.0001.

Bacteroidota ratio, whereas these alterations were attenuated following SMEVs treatment (Figure 4A). At the family level, the relative abundance of Enterobacteriaceae was increased in the model group, while Lactobacillaceae and Muribaculaceae were reduced. These changes showed opposite trends after SMEVs administration (Figure 4B). At the genus level, increased abundances of Klebsiella and Lachnoclostridium, along with a marked reduction in Ligilactobacillus, were observed in the model group; these alterations were partially reversed following SMEVs treatment (Figure 4C).

Microbial diversity analyses further demonstrated changes in community structure. Venn diagram analysis identified a total of 677 shared amplicon sequence variants (ASVs among the control, model, and SMEVs-treated groups (Figure 5A). α-diversity analysis showed that SMEVs treatment increased the Shannon and Simpson indices in DKD mice (Figure 5B). β-diversity analysis based on unweighted UniFrac distance (R=0.32, P=0.001) and weighted UniFrac distance (R=0.401, P=0.002) revealed a clear separation between the control and model groups, whereas the microbial community structure of the SMEVs-treated group showed a higher degree of overlap with that of the control group (Figure 5C and D). Further linear discriminant analysis effect size (LEfSe) analysis identified distinct taxonomic features among groups. Differences between the control and model groups were mainly associated with taxa within the phylum Bacteroidota, including the class Bacteroidia, order Bacteroidales, and the families Muribaculaceae, Prevotellaceae, and Rikenellaceae. In contrast, differential taxa between the model and SMEVs-treated groups were primarily enriched within the phyla Desulfobacterota and Bacteroidota (Figure 5E–G). Collectively, these results indicate that SMEVs treatment altered gut microbiota composition and community structure in DKD mice.

Effects of SMEVs on Gut Metabolomic Profiles in DKD Mice

To evaluate the effects of SMEVs on gut metabolomic profiles in DKD mice, an untargeted metabolomics approach was applied to intestinal content samples. A total of 6166 metabolites were identified, which were mainly classified as lipids and lipid-like molecules (31.58%), organic acids and derivatives (24.94%), Organoheterocyclic compounds (13.36%), and benzenoid (12.49%) (Figure 6A). Differential metabolite analysis revealed 359 metabolites that differed between the model and control groups, 461 metabolites between the model and SMEVs-treated groups, and 367 metabolites between the control and SMEVs-treated groups (Figure 6B). PCA demonstrated a clear separation between the control and model groups in the principal component space, while the SMEVs-treated group was distributed between these two groups and showed a clustering trend closer to the control group (Figure 6C–F). OPLS-DA further revealed distinct separation of

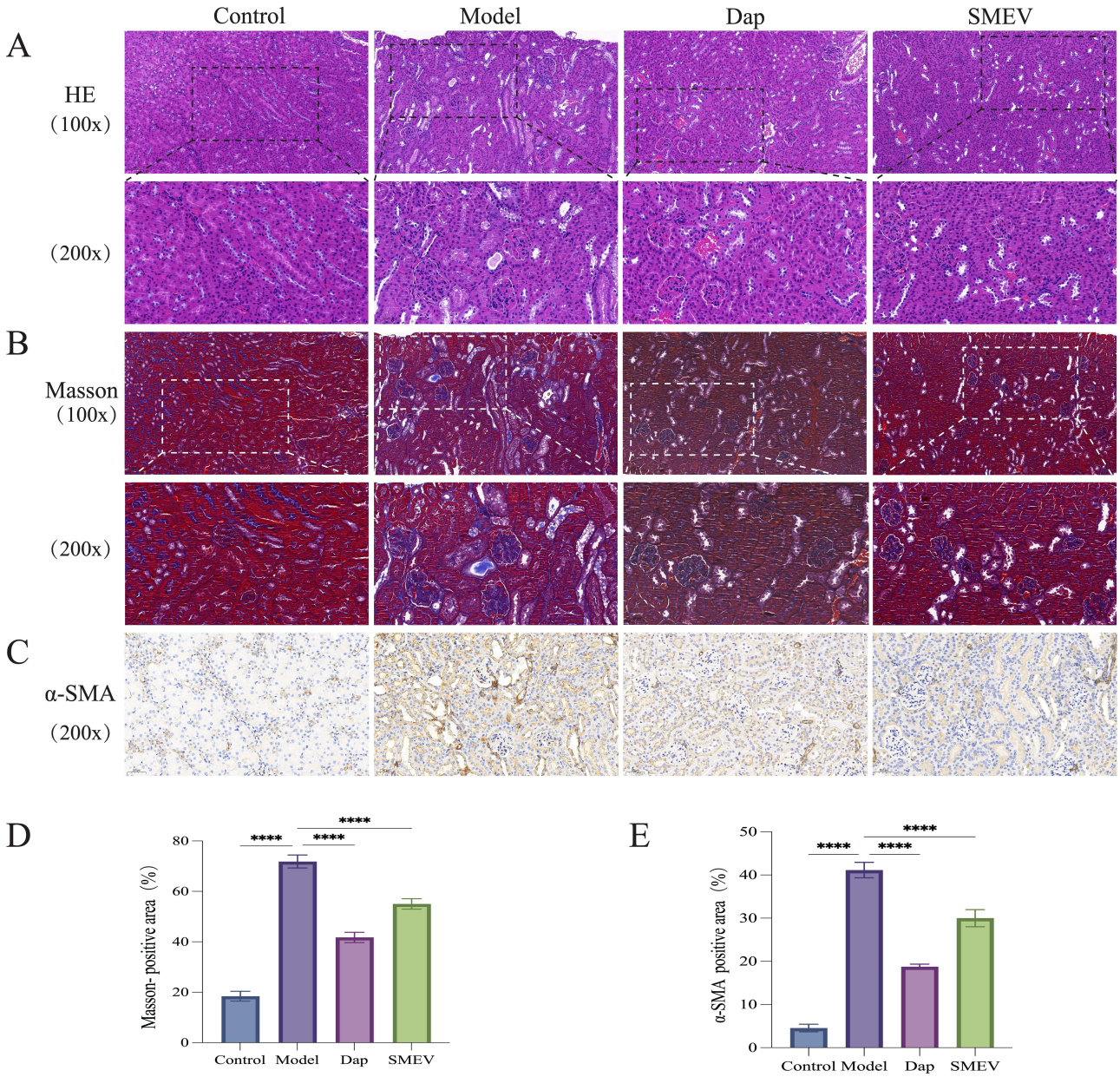

Figure 3 Effects of SMEVs on Renal Histopathological Injury and Fibrosis in DKD Mice. (**A**) HE staining of renal tissues (X100.Scale bar: 100 μm; X200.Scale bar: 50 μm). (**B**) Masson staining of renal tissues (X100.Scale bar: 100 μm; X200.Scale bar: 50 μm). (**C**) Immunohistochemistry of renal tissues (X200.Scale bar: 50 μm). (**D**) The ratio of Masson staining positive area; (**E**) The ratio of Immunohistochemistry staining positive area. Data are presented as mean±SD (n=6 mice per group). ****p<0.0001.

metabolomic profiles among groups, indicating significant metabolic differences between the control and model groups as well as between the model and SMEVs-treated groups (Figure 6G and H). Consistently, hierarchical clustering heatmaps showed distinct metabolite expression patterns between the model and control groups, whereas the metabolomic profile of the SMEVs-treated group differed from that of the model group across most metabolites (Figure 6I–K).

Volcano plots were used to further visualize the distribution of differential metabolites between groups (Figure 7A and B). Hierarchical clustering analysis of differential metabolites showed distinct expression patterns between the model and control groups, while the SMEVs-treated group exhibited a metabolite expression profile that was distinguishable from the model group (Figure 7C and D). Among the differential metabolites between the control and model groups, the top 20 metabolites ranked by variable importance in projection (VIP) scores included 11,12-DHET, 7-dehydrocholesterol, PE-NMe (18:0, 18:0), PC (18:1, 16:1), and 4-methylzymosterol (Figure 7E and F). In contrast, the top 20 differential metabolites between the model

https://doi.org/10.2147/IJN.S580968

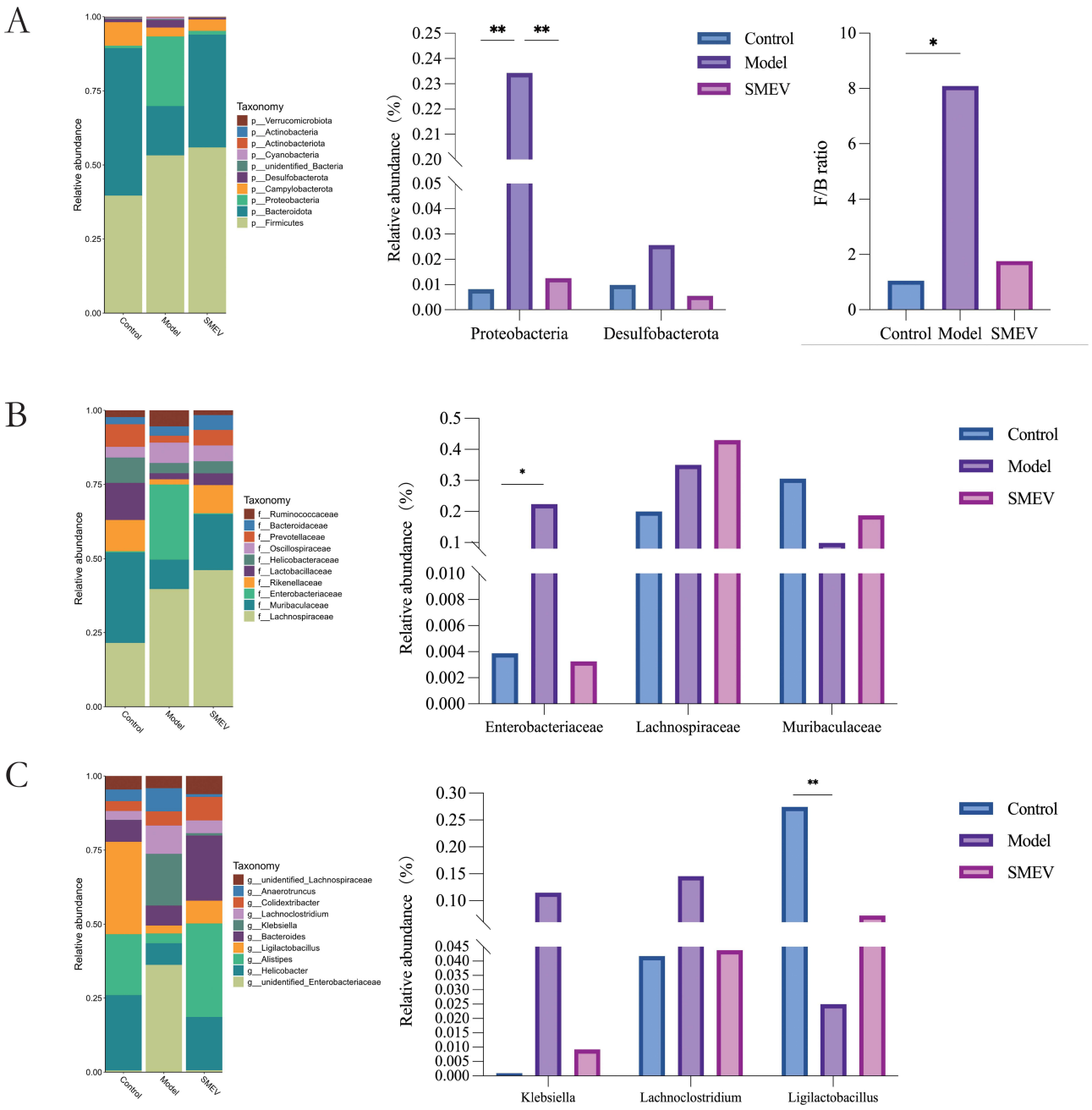

Figure 4 Effects of SMEVs on the gut microbiota composition in mice with DKD. (**A**) Relative abundance of gut microbiota at the phylum level. (**B**) Relative abundance at the family level. (**C**) Relative abundance at the genus level. Data are presented as relative abundance. n=6 mice per group. *p<0.05, **p<0.01.

and SMEVs-treated groups included Ile-Glu-Asn, Gly-His-Gly, Pro-Trp, PC (14:0_22:0), petroselinic acid, 11-oxohexadecanoic acid, and Tyr-Leu-His (Figure 7G and H). KEGG pathway enrichment analysis of differential metabolites between the control and model groups indicated significant enrichment in linoleic acid metabolism, retrograde endocannabinoid signaling, primary bile acid biosynthesis, and arachidonic acid metabolism (Figure 7I). In comparison, KEGG enrichment analysis between the model and SMEVs-treated groups showed that differential metabolites were mainly involved in ovarian steroidogenesis, inflammatory mediator regulation of transient receptor potential (TRP) channels, and C5-branched dibasic acid metabolism (Figure 7J). Collectively, these results demonstrate that SMEVs intervention significantly altered the gut metabolomic profiles in DKD mice.

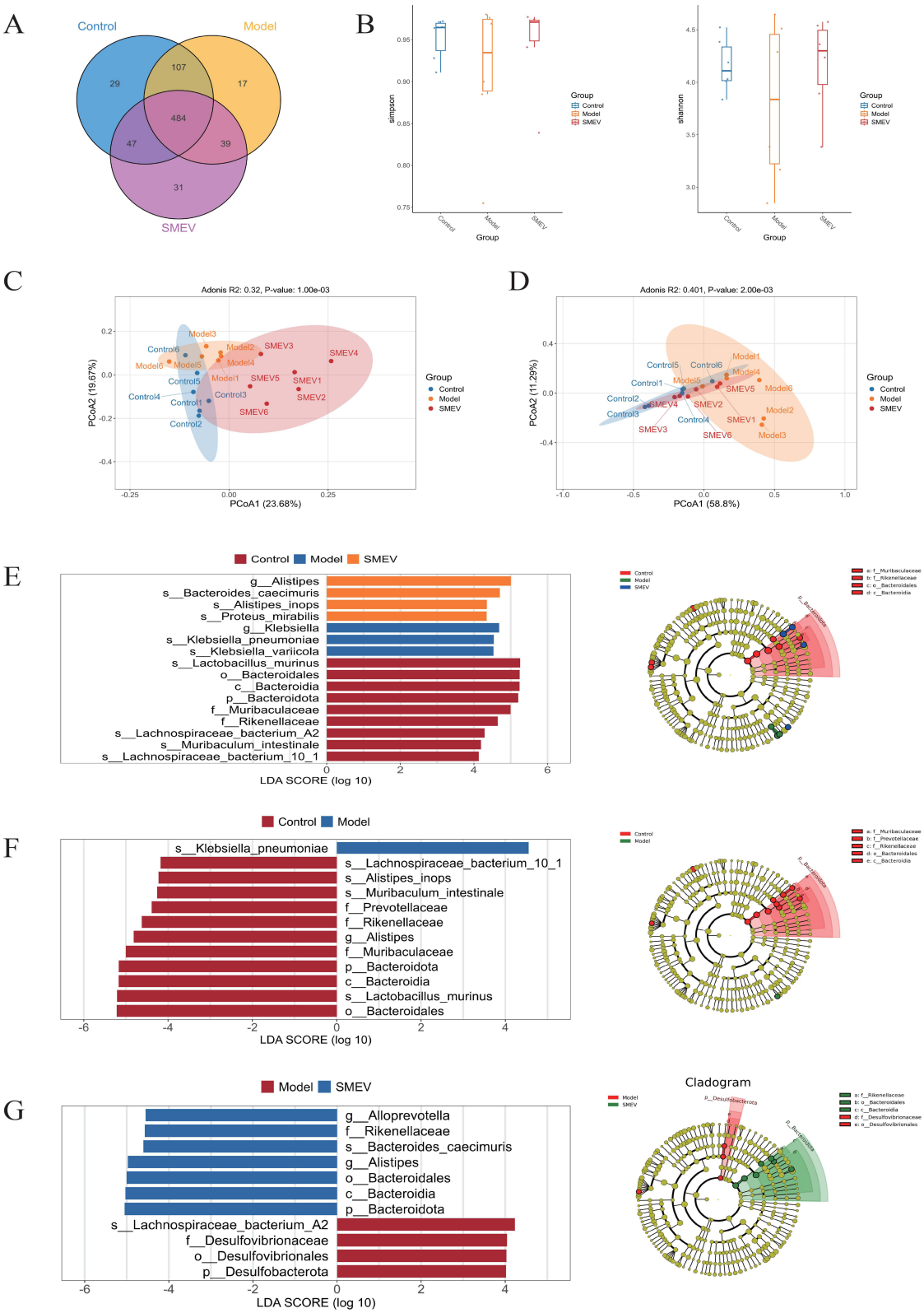

Figure 5 Effects of SMEVs on gut microbial diversity and differential taxa in DKD mice. (**A**) Venn diagram showing shared and unique ASVs among groups. (**B**) Alpha diversity indices (Shannon and Simpson). (**C**) Beta diversity analysis based on unweighted UniFrac distances, visualized by PCoA. (**D**) Beta diversity analysis based on weighted UniFrac distances, visualized by PCoA. (**E**) LEfSe analysis identifying differentially abundant taxa among the control, model, and SMEVs-treated groups. (**F**) LEfSe analysis identifying differentially abundant taxa between the control and model groups. (**G**) LEfSe analysis identifying differentially abundant taxa between the model and SMEVs-treated groups. n=6 mice per group.

https://doi.org/10.2147/IJN.S580968

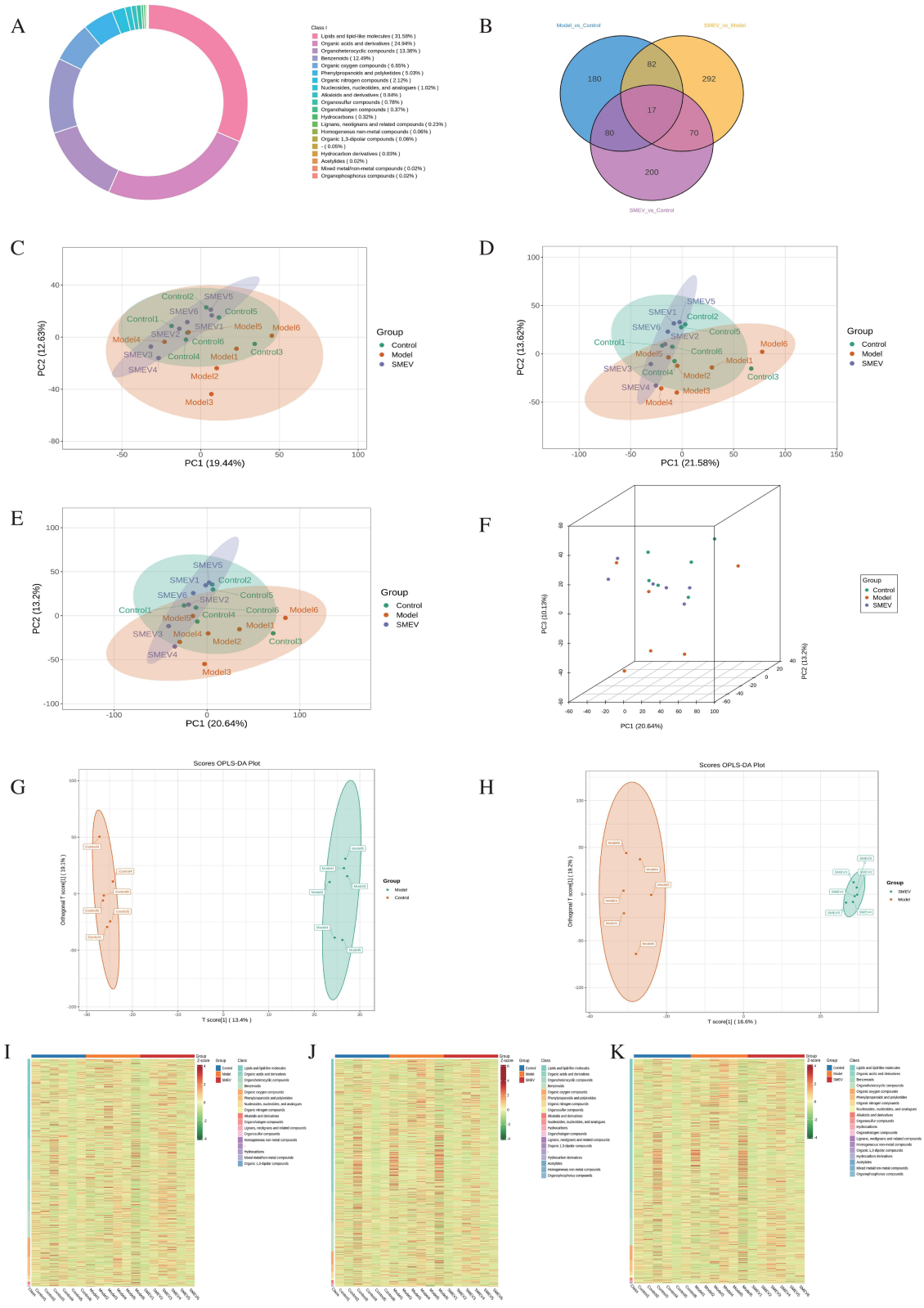

Figure 6 Effects of SMEVs on gut metabolomic profiles in DKD mice. (**A**) Classification of detected metabolites. (**B**) Venn diagram of differential metabolites among groups. (**C**–**E**) Two-dimensional PCA score plots of gut metabolomic profiles under negative ion mode (**C**), positive ion mode (**D**), and integrated ion mode (**E**). (**F**) Three-dimensional PCA score plot based on the integrated metabolomic dataset. (**G**) OPLS-DA model with permutation testing comparing the control and model groups. (**H**) OPLS-DA model with permutation testing comparing the model and SMEVs-treated groups. (**I**–**K**) Hierarchical clustering heatmaps of metabolites identified under negative ion mode (**I**), positive ion mode (**J**), and integrated ion mode (**K**). n=6 mice per group.

Correlation Analysis Between Gut Microbiota and Differential Metabolites in DKD Mice

To explore the potential interactions between gut microbiota and metabolic alterations, an integrated correlation analysis was performed between bacterial abundances at the family level and differential metabolites using Spearman correlation analysis. Significant correlations were defined as |r|>0.5 with $P<0.05$ and were visualized as a heatmap (Figure 8A). The results showed that members of the phylum Bacteroidota, particularly the family Muribaculaceae and its representative species *Muribaculum intestinale*, were positively correlated with multiple lipid and sterol-related metabolites, including PE-NMe (18:0_18:0), PC (20:1_18:1), and sterculic acid. In contrast, these taxa were negatively correlated with the inflammation-associated metabolite 11,12-DiHETrE. Similarly, the Bacteroidota family Rikenellaceae and the genus Alistipes were positively correlated with phospholipid-related metabolites, such as PE-NMe (18:0_15:0), while showing negative correlations with oxidized lipids (eg, 11,12-DiHETrE) and aromatic metabolites, including 2-(4-methylphenyl)-1-propanol. In addition, Lactobacillus murinus belonging to the phylum Firmicutes exhibited positive correlations with several antioxidant-related metabolites, including daucol, pinosylvin methyl ether, and arabinonic acid, whereas a negative correlation was observed with allopumiliotoxin 267a. In contrast, members of the phylum Proteobacteria, particularly the genus Klebsiella (including *K. variicola* and *K. pneumoniae*), showed negative correlations with lipid

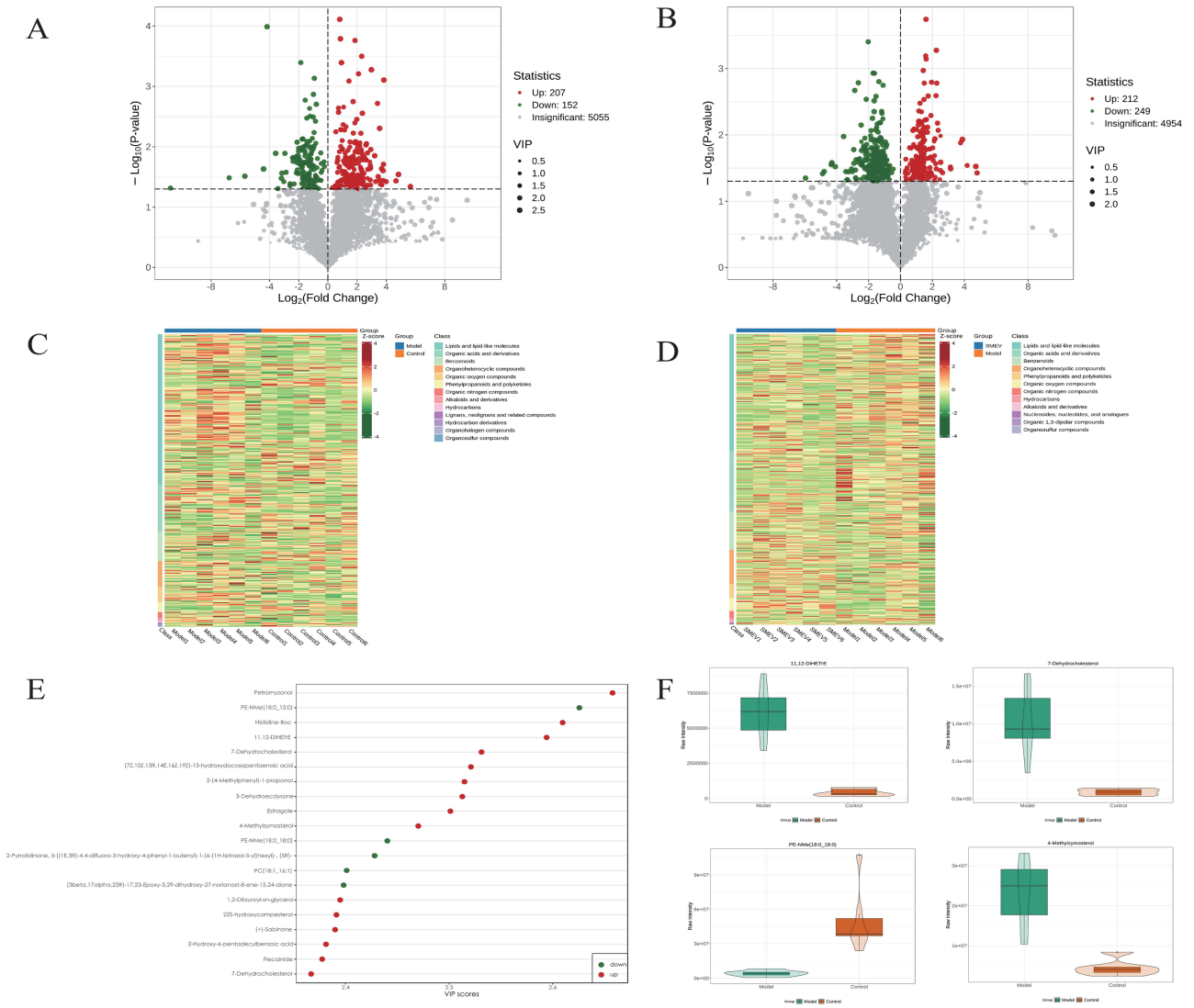

Figure 7 continued.

https://doi.org/10.2147/IJN.S580968

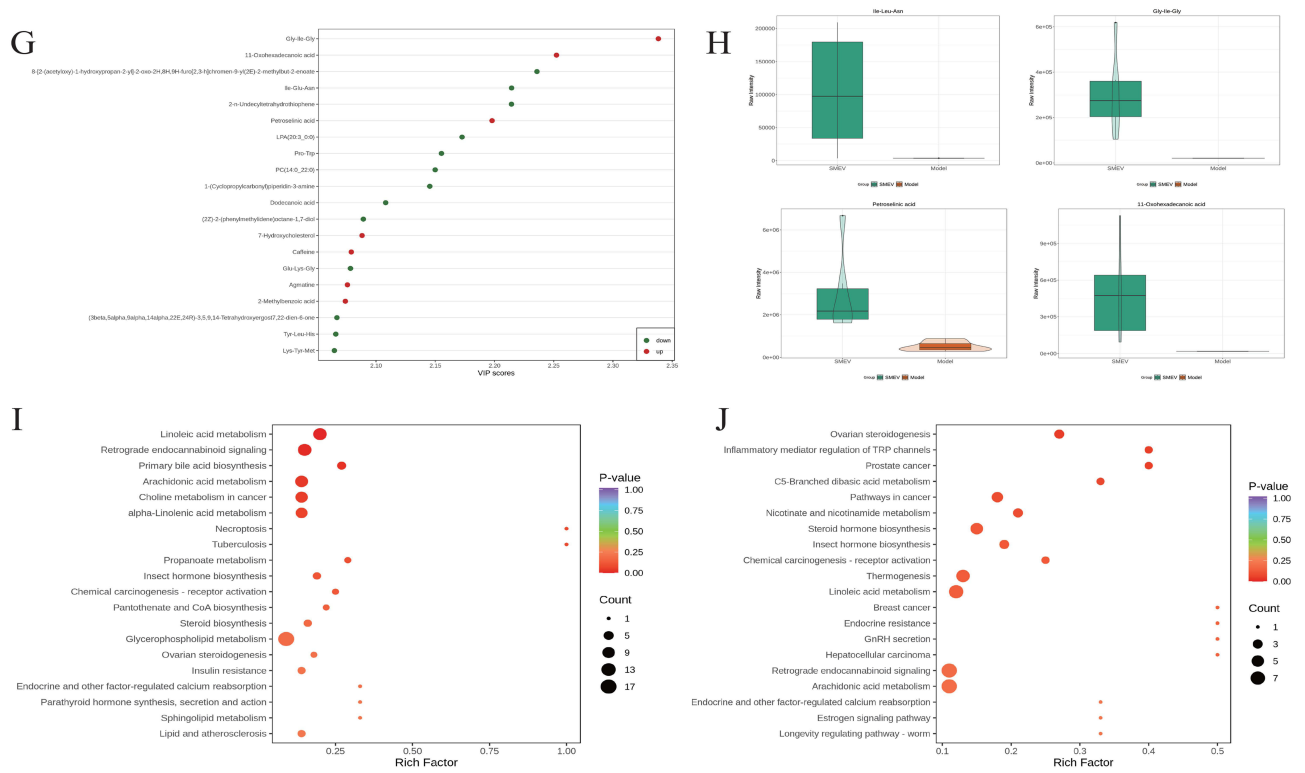

Figure 7 Differential metabolite analysis and KEGG pathway enrichment in DKD mice after SMEVs treatment. (**A**) Volcano plot showing differential metabolites between the control group and model group. (**B**) Volcano plot showing differential metabolites between the model group and SMEVs-treated group. (**C**) Hierarchical clustering heatmaps of differential metabolites identified between control and model groups. (**D**) Hierarchical clustering heatmaps of differential metabolites identified between model and SMEVs-treated groups. (**E**) Top 20 metabolites ranked by VIP scores between the control group and model group. (**F**) Violin plots of representative differential metabolites between the control group and model group. (**G**) Top 20 metabolites ranked by VIP scores between the model group and SMEVs-treated group. (**H**) Violin plots of representative differential metabolites between the model group and SMEVs-treated group. (**I**) KEGG pathway enrichment analysis of differential metabolites between the control group and model group. (**J**) KEGG pathway enrichment analysis of differential metabolites between the model group and SMEVs-treated group. Differential metabolites were defined by VIP>1 and $p<0.05$. n=6 mice per group.

metabolites such as PA (20:0_19:0) and Riesling acetal, but positive correlations with amino acid-derived metabolites (eg, Leu-Glu-Ile) and sterol intermediates, including 4,4-dimethyl-8,24-cholestadienol. To further highlight robust microbiota–metabolite associations, correlations with $|r|>0.8$ and $P<0.05$ were selected for chord diagram analysis (Figure 8B). This analysis revealed characteristic associations between representative taxa and key metabolic pathways: Lactobacillus murinus was negatively correlated with the terpenoid metabolite phytol; Rikenellaceae and Alistipes were negatively correlated with isoprenoid and polyisoprenoid metabolites, including D-trans-and poly-cis-undecaprenyl diphosphate; whereas Muribaculum intestinale showed a positive correlation with the unsaturated fatty acid metabolite 7,7-dimethyl-(5Z,8Z)-eicosadienoic acid and negative correlations with peptide metabolites such as Leu-Ser and lipid-derived metabolites including 11,12-DiHETrE. Correlation scatter plots further illustrated the relationships between representative differential taxa and key metabolites across groups (Figure 8C).

Discussion

Although the management of DKD has improved in recent years through integrated interventions such as glycemic control, blood pressure regulation, and inhibition of the renin–angiotensin system, disease progression remains difficult to halt in a substantial proportion of patients. Current therapeutic strategies primarily target hemodynamic alterations or metabolic disturbances, but are less effective in addressing deeper pathogenic processes, including inflammation, oxidative stress, and gut microbial dysbiosis. Consequently, irreversible deterioration of renal function still occurs in some patients despite standardized treatment.[3] These limitations suggest that key pathological drivers of DKD remain incompletely understood and highlight the need for therapeutic approaches capable of simultaneously targeting metabolic imbalance, inflammatory

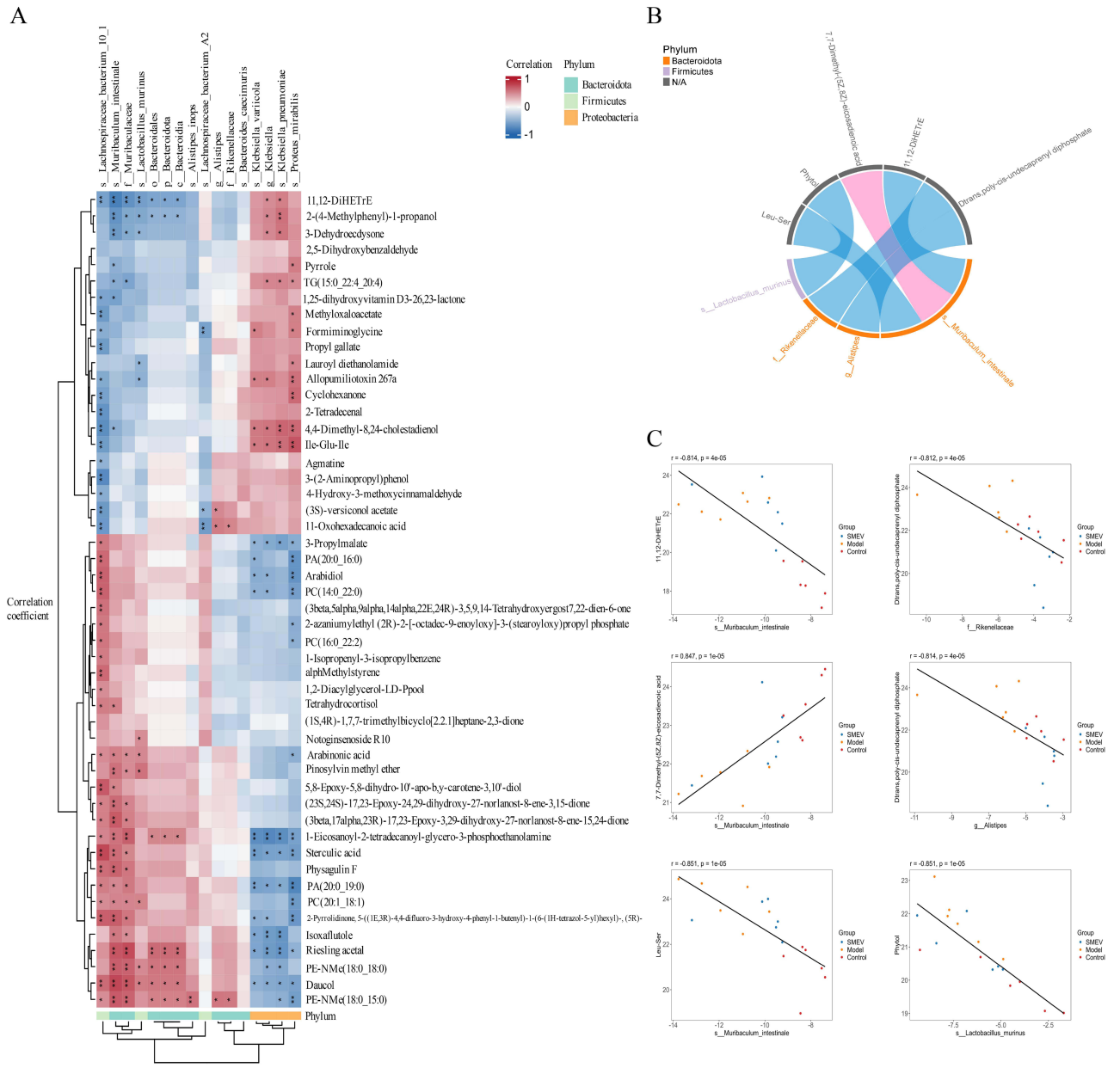

Figure 8 Correlation analysis between gut microbiota and differential metabolites in DKD mice. (**A**) Hierarchical clustering heatmap based on Spearman correlation analysis. (**B**) Chord diagram illustrating significant microbiota–metabolite associations. (**C**) Scatter plots showing representative correlations. Only correlations with |r|>0.5 and $p<0.05$ were included. n=6 mice per group. $p<0.05$ was considered statistically significant (*), and $p<0.01$ highly significant (**).

responses, and microbial dysregulation. PDEVs, as orally administrable and cross-kingdom natural nanocarriers, have not yet been extensively explored in the context of DKD. In the present study, ex vivo fluorescence imaging revealed pronounced enrichment of orally administered SMEVs in the intestinal region. This distribution pattern suggests that SMEVs exhibit gastrointestinal stability and remain detectable in the gut following oral administration rather than being rapidly degraded or eliminated. Such intestinal retention enables SMEVs to interact with the gut microbiota and potentially influence downstream microbially derived metabolites. Therefore, gastrointestinal stability and preferential intestinal retention represent key advantages underlying the therapeutic potential of orally administered SMEVs. Beyond their physical stability and biodistribution, our recent studies involving chemical composition profiling and microRNA (miRNA) sequencing revealed that SMEVs carry *Salvia miltiorrhiza*–associated bioactive constituents and are enriched in a series of conserved plant-derived miRNAs. Functional enrichment analyses indicated that these miRNAs are involved in pathways

https://doi.org/10.2147/IJN.S580968

related to signal transduction and metabolic regulation, with reported roles in maintaining endothelial barrier integrity, modulating inflammatory responses, and promoting vascular repair.[23] In the present study, Coomassie brilliant blue staining further confirmed that SMEVs contain abundant protein components, suggesting that SMEVs may also participate in host- or microbiota-related signaling processes through protein delivery. Collectively, these findings support the notion that SMEVs may act as vesicle-mediated carriers that coordinately deliver miRNAs, proteins, and lipophilic phytochemicals, thereby exerting biological effects at multiple regulatory levels. Previous studies have shown that plant-derived extracellular vesicles can reshape gut microbial community structure by modulating the host mucosal microenvironment.[24] Accordingly, we propose that, in the context of DKD, orally administered SMEVs are capable of delivering miRNAs and lipophilic phytochemicals to the intestinal lumen and mucosa, thereby modulating gut microbial ecology and reshaping microbially derived metabolic profiles, including metabolites associated with oxidative stress and inflammatory signaling. These effects may contribute to the observed attenuation of renal inflammation and improvement in metabolic homeostasis. Nevertheless, the specific microbial targets of SMEV-derived miRNAs and proteins, as well as the host signaling pathways involved, remain to be elucidated and warrant further investigation. Overall, this study provides systematic evidence, from the perspective of gut microecology and metabolic regulation, that SMEVs may ameliorate DKD pathology through modulation of the gut–kidney axis, thereby offering an experimental foundation for the development of a biologically active and safe oral therapeutic strategy.

Disruption of glucose and lipid metabolism promotes renal structural remodeling and accelerates renal functional decline by activating inflammatory mediators and profibrotic signaling pathways, such as transforming growth factor-β1 (TGF-β1) and nuclear factor-κB (NF-κB).[25] Previous studies have demonstrated that restoration of glucose and lipid metabolic homeostasis can effectively delay the progression of DKD.[26] In the present study, SMEVs intervention significantly improved metabolic abnormalities and renal dysfunction in DKD mice, as evidenced by reductions in fasting blood glucose and triglyceride levels, partial recovery of body weight, and decreases in proteinuria, urinary albumin-to-creatinine ratio, serum creatinine, blood urea nitrogen, and uric acid levels. Histopathological analyses further revealed that SMEVs treatment alleviated glomerular and tubular structural damage and reduced collagen deposition, indicating attenuation of renal fibrosis. Collectively, these findings demonstrate a consistent association between SMEVs-mediated improvement of glucose and lipid metabolic disturbances and the amelioration of renal structural and functional injury, suggesting that SMEVs may contribute to DKD improvement through modulation of metabolic imbalance, inflammatory responses, and oxidative stress–related processes.

The gut microbiota is a critical regulator of host metabolic homeostasis, and alterations in its composition and metabolic activity can profoundly influence systemic energy metabolism and immune balance. Accumulating evidence has demonstrated that gut microbial dysbiosis is closely associated with diabetes mellitus and its chronic complications.[4] In DKD, microbial imbalance not only contributes to disturbances in glucose and lipid metabolism but also promotes inflammatory responses and renal tissue injury through increased endotoxin load and impaired intestinal barrier function.[5] Enhanced intestinal permeability and microbial dysbiosis facilitate the translocation of metabolic toxins and inflammatory mediators into the circulation, thereby altering the local renal immune microenvironment and influencing stress responses and fibrotic processes in tubular epithelial cells.[6] Under physiological conditions, certain commensal bacteria maintain intestinal barrier integrity, alleviate oxidative stress, and suppress inflammatory signaling through the production of SCFAs. In contrast, opportunistic pathogenic taxa, particularly those within the phylum Proteobacteria, release lipopolysaccharide (LPS), which activates the TLR4/NF-κB pathway and induces inflammatory responses.[27,28] In addition, gut-derived secondary bile acids participate in the regulation of lipid and energy metabolism via FXR/TGR5 signaling, and their dysregulation has been implicated in the development of renal fibrosis.[29] Emerging evidence further suggests that gut-derived extracellular vesicles can interact with microbial gene expression or indirectly reshape microbial community structure by modulating the host mucosal microenvironment.[30] Accordingly, restoration of gut microbial homeostasis has emerged as an important therapeutic strategy for improving DKD progression. In the present study, DKD mice exhibited increased relative abundances of Proteobacteria, Enterobacteriaceae, and Klebsiella, taxa that have been linked to endotoxin production, TLR4 activation, and chronic low-grade inflammation, and are considered potential risk-associated microbes in metabolic disorders and chronic kidney disease.[7,31] In contrast, SMEVs intervention restored the abundance of beneficial taxa such as Muribaculaceae and Lachnospiraceae, which are commonly associated

with SCFA production, maintenance of intestinal barrier function, and attenuation of inflammatory responses.[32] Diversity analyses further supported these observations: reduced α-diversity in DKD mice indicated compromised microbial stability and metabolic capacity,[19] whereas SMEVs treatment increased α-diversity and shifted β-diversity closer to that of the control group, suggesting a global remodeling of the gut microbial community. LEfSe analysis revealed a marked reduction in Desulfobacterota, particularly Desulfovibrionaceae, following SMEVs intervention. This group of sulfate-reducing bacteria has been shown to disrupt tight junction integrity and exacerbate inflammatory burden, exhibiting pathogenic features in multiple metabolic disease models.[33] Concurrently, the re-establishment of Bacteroidota as a dominant phylum may facilitate carbohydrate utilization and SCFA production, thereby contributing to the modulation of inflammation-related metabolic pathways.[34] Collectively, these findings indicate that SMEVs reduce the abundance of bacteria associated with inflammation and barrier disruption while promoting the recovery of SCFA-producing beneficial taxa. The SMEVs-induced improvements in gut microbial composition and diversity are consistent with the observed attenuation of renal pathological injury in DKD mice, suggesting that gut microbial remodeling may provide an important biological context for the renoprotective effects of SMEVs.

Gut-derived metabolites are increasingly recognized as critical mediators linking the intestinal microbiota to host metabolic homeostasis and play essential roles in the development and progression of diabetes mellitus and DKD. Lipids, amino acids, and their derivatives originating from the gut can influence renal pathology by modulating inflammatory responses, oxidative stress, and fibrosis-related signaling pathways.[5] Among these alterations, dysregulated lipid metabolism represents a central component of metabolic disturbances in DKD.[35] Therefore, characterizing changes in the gut metabolic profile following SMEVs intervention provides important mechanistic insight into its protective effects against DKD. In the present study, untargeted metabolomic analysis revealed significant alterations in multiple lipid-related metabolic pathways in the intestinal contents of DKD mice. Specifically, levels of the arachidonic acid metabolite 11,12-DHET and several phospholipid species were significantly elevated in DKD mice. These metabolites are closely associated with activation of pro-inflammatory signaling pathways and enhanced oxidative stress. Previous studies have demonstrated that 11,12-DHET, a downstream product of arachidonic acid metabolism, participates in the regulation of inflammatory responses and promotes tubulointerstitial injury, with elevated levels frequently correlating with aggravated renal inflammation and fibrosis.[36] Concurrently, abnormal accumulation of phospholipids and lysophospholipids reflects disruption of membrane lipid homeostasis, which can amplify membrane stress responses and oxidative damage, thereby exacerbating tubular epithelial dysfunction and structural renal injury.[37,38] KEGG pathway enrichment analysis further indicated significant activation of arachidonic acid metabolism, linoleic acid metabolism, and primary bile acid biosynthesis under DKD conditions. These findings suggest that sustained enhancement of pro-inflammatory lipid signaling and bile acid metabolic imbalance may jointly contribute to pathological regulation of the gut–kidney metabolic axis by influencing inflammatory responses, oxidative stress, and lipid homeostasis. Aberrant activation of these metabolic pathways thus provides an important metabolic basis for inflammation amplification and fibrotic progression in DKD. Notably, SMEVs intervention restored or upregulated several metabolites with potential protective properties, including the bioactive peptide Tyr–Leu–His and the unsaturated fatty acid petroselinic acid. Previous studies suggest that small bioactive peptides such as Tyr–Leu–His may improve the oxidative stress microenvironment by enhancing antioxidant enzyme activity and scavenging excessive free radicals,[39] thereby attenuating oxidative stress–associated inflammatory signaling. Petroselinic acid, a monounsaturated fatty acid with anti-inflammatory and membrane-stabilizing properties, may help restore membrane lipid composition, reduce lipotoxicity and membrane stress, and protect tubular epithelial cells from sustained metabolic stress.[40] Consistently, KEGG analysis showed that SMEVs treatment modulated pathways related to inflammatory mediator regulation and lipid signal transduction, while simultaneously influencing multiple amino acid–related metabolic pathways. Amino acids and their derivatives play important roles in maintaining redox balance, suppressing apoptosis, and preserving renal function, and reductions in their levels are commonly associated with renal functional deterioration.[41] Therefore, regulation of amino acid metabolism by SMEVs may support their renoprotective effects by improving antioxidant capacity and cellular metabolic adaptability. Collectively, these findings indicate that SMEVs ameliorate DKD-associated metabolic abnormalities by correcting lipid metabolic imbalance, restoring amino acid and peptide metabolites with antioxidant and membrane-protective properties, and suppressing lipid signaling pathways closely linked to inflammation and oxidative stress. This metabolic remodeling

—centered on the lipid–oxidative stress–inflammation–fibrosis axis—may constitute a fundamental mechanistic basis for the observed attenuation of renal inflammation and interstitial fibrosis in DKD mice following SMEVs treatment.

Spearman correlation analysis revealed significant associations between alterations in gut microbial composition and fluctuations in multiple classes of metabolites, suggesting that SMEVs may exert protective effects through modulation of the gut–kidney axis. Following SMEVs intervention, enriched taxa including Muribaculaceae, Rikenellaceae, and Lactobacillus murinus showed positive correlations with various lipid metabolites, membrane-stabilizing compounds, and antioxidant-related molecules, such as daucol, PE-NMe species, phosphatidylcholine (PC) species, and several unsaturated fatty acid derivatives. These metabolites are largely involved in lipid metabolic regulation, buffering of oxidative stress, and maintenance of cellular membrane homeostasis, indicating that SMEVs-induced microbial remodeling may be accompanied by an improved intestinal lipid metabolic environment. Muribaculaceae, recognized as an important polysaccharide-degrading and SCFA-producing bacterial family, has been shown to enhance energy supply to the intestinal epithelium, reinforce barrier integrity, and reduce gut-derived inflammatory burden.[32] In the present study, Muribaculaceae abundance was positively correlated with multiple phospholipids and unsaturated fatty acid metabolites, suggesting that this taxon may participate in SMEVs-mediated restoration of lipid homeostasis. Concurrently, increased levels of lipid metabolites with anti-inflammatory and membrane-stabilizing properties, such as daucol and sterculic acid, may reflect a reduction in intestinal oxidative stress burden and a shift of the gut–kidney metabolic axis toward a more homeostatic state. Previous studies have demonstrated that such metabolites can alleviate lipotoxic injury to renal tubular epithelial cells.[42] Therefore, enrichment of Muribaculaceae and its coordinated changes with these metabolites not only indicate improved microbial ecology but may also be linked to restoration of renal-associated lipid metabolic balance. In addition, Lactobacillus murinus exhibited significant positive correlations with daucol, PE-NMe (18:0_18:0), PC (20:1_18:1), and the antioxidant compound pinosylvin methyl ether. Members of the Lactobacillus genus are known to influence host lipid profiles and attenuate inflammatory responses indirectly through SCFAs production and modulation of bile acid metabolism.[43] Accordingly, the observed correlations between Lactobacillus murinus and phospholipid as well as antioxidant metabolites suggest that SMEVs may promote recovery of antioxidant capacity and membrane-stabilizing metabolic processes within the gut–kidney metabolic network by increasing the abundance of this beneficial taxon. Conversely, Proteobacteria and its representative genus Klebsiella (including *K. variicola* and *K. pneumoniae*) showed negative correlations with beneficial metabolites such as daucol, sterculic acid, and PA (20:0_19:0), while displaying positive correlations with metabolites potentially associated with pro-inflammatory signaling or metabolic dysregulation, including Leu–Glu–Ile and 4,4-dimethyl-8,24-cholestadienol. As a typical opportunistic pathogen, excessive proliferation of Klebsiella can disrupt intestinal barrier integrity and induce systemic low-grade inflammation, and has been implicated as a risk factor for DKD progression.[44] The reduction of Klebsiella abundance following SMEVs treatment, together with concomitant upregulation of intestinal phospholipids and antioxidant metabolites, further supports the notion that SMEVs may improve gut–kidney metabolic homeostasis by suppressing pathogen-associated metabolic pathways. Notably, the arachidonic acid metabolite 11,12-DiHETrE was negatively correlated with several health-associated taxa, including Muribaculaceae, while showing a positive correlation with Klebsiella. This metabolite is considered an important pro-inflammatory lipid mediator, and previous studies have demonstrated its involvement in enhanced oxidative stress and fibrotic responses in renal tissue.[45] These findings suggest that SMEVs may attenuate DKD-associated inflammation and fibrosis by reshaping the gut microbial structure and suppressing aberrant activation of arachidonic acid metabolic pathways. Collectively, SMEVs regulate the gut microbiota–metabolite axis at multiple levels: on one hand, they promote the recovery of beneficial taxa such as Muribaculaceae and Lactobacillus, thereby enhancing lipid and antioxidant-related metabolic pathways; on the other hand, they suppress opportunistic pathogens such as Klebsiella and their associated pro-inflammatory metabolic signatures, leading to reduced levels of inflammatory lipid mediators. This coordinated modulation of microbial ecology and metabolism may alleviate endotoxin burden and inflammatory signaling at the systemic level, thereby providing an important metabolic basis for the attenuation of renal injury and interstitial fibrosis associated with DKD.

Conclusion

Through a combination of animal experiments,16S rRNA sequencing, and untargeted metabolomic analyses, the present study demonstrates the beneficial effects of orally administered SMEVs on the progression of DKD and suggests that the protective effects may be mediated, at least in part, through remodeling of the gut microbiota and associated metabolomic profiles. Our findings indicate that SMEVs may delay DKD progression by modulating key components and functional characteristics of the gut microbiota, thereby contributing to a deeper understanding of the complex interactions between DKD and the host microbial ecosystem. As a naturally derived, orally administrable, and cross-kingdom extracellular vesicle system, SMEVs exhibit promising translational potential. Further studies are warranted to validate the specific interactions between SMEVs and the gut microbiota and to clarify their causal roles in disease modulation, which may ultimately facilitate the development of more targeted and effective strategies for the prevention and management of DKD.

Abbreviations

DKD, diabetic kidney disease; DM, Diabetes mellitus; SMEV, *Salvia miltiorrhiza*-derived Extracellular Vesicle; ESRD, end-stage renal disease; TEM, transmission electron microscope; NTA, nanoparticle tracking analysis; SCFAs, short-chain fatty acids; LPS, lipopolysaccharide; UACR, Urine Albumin-to-Creatinine Ratio; BUN, Blood Urea Nitrogen; CREA, Creatinine; UA, Blood uric acid; TG, Triglyceride; OPLS-DA, Orthogonal Partial Least Squares-Discriminant Analysis; PCA, Principal Component Analysis; MOD, Mean Optical Density; HE, Hematoxylin–Eosin; BCA, bicinchoninic acid; IHC, Immunohistochemistry; miRNA, microRNA.

Acknowledgments

The authors sincerely thank Professor Li Ling from the Institute of Innovation and Applied Research in Chinese Medicine, Hunan University of Chinese Medicine, for her valuable technical support and expert guidance during this study.

Funding

This work was supported by grants from the guiding project of the "Academician Liu Liang Workstation" (No: 24YS003), National Natural Science Foundation of China (No: U21A2041), Hunan Provincial Natural Science Foundation Innovation Research Group Project (No: 2024JJ1007), The Youth Student Basic Research Project of the Natural Science Foundation of Hunan Province (No:2026JJ90291).

Disclosure

The author(s) report no conflicts of interest in this work.

References

1. Tuttle KR, Agarwal R, Alpers CE, et al. Molecular mechanisms and therapeutic targets for diabetic kidney disease. *Kidney Int*. 2022;102(2):248–260. doi:10.1016/j.kint.2022.05.012
2. Thipsawat S. Early detection of diabetic nephropathy in patient with type 2 diabetes mellitus: a review of the literature. *Diab Vasc Dis Res*. 2021;18(6):14791641211058856. doi:10.1177/14791641211058856
3. Fu H, Liu S, Bastacky SI, Wang X, Tian XJ, Zhou D. Diabetic kidney diseases revisited: a new perspective for a new era. *Mol Metab*. 2019;30:250–263. doi:10.1016/j.molmet.2019.10.005
4. Jiao Y, Wu L, Huntington ND, Zhang X. Crosstalk between gut microbiota and innate immunity and its implication in autoimmune diseases. *Front Immunol*. 2020;11:282. doi:10.3389/fimmu.2020.00282
5. Wu IW, Liao YC, Tsai TH, et al. Machine-learning assisted discovery unveils novel interplay between gut microbiota and host metabolic disturbance in diabetic kidney disease. *Gut Microbes*. 2025;17(1):2473506. doi:10.1080/19490976.2025.2473506
6. Chen YY, Chen DQ, Chen L, et al. Microbiome-metabolome reveals the contribution of gut-kidney axis on kidney disease. *J Transl Med*. 2019;17(1):5. doi:10.1186/s12967-018-1756-4
7. Wang Y, Zhao J, Qin Y, et al. The specific alteration of gut microbiota in diabetic kidney diseases-a systematic review and meta-analysis. *Front Immunol*. 2022;13:908219. doi:10.3389/fimmu.2022.908219
8. Mao ZH, Gao ZX, Liu DW, Liu ZS, Wu P. Gut microbiota and its metabolites - molecular mechanisms and management strategies in diabetic kidney disease. *Front Immunol*. 2023;14:1124704. doi:10.3389/fimmu.2023.1124704
9. Cheng TO. Danshen: a popular Chinese cardiac herbal drug. *J Am Coll Cardiol*. 2006;47(7):1498. doi:10.1016/j.jacc.2006.01.001
10. Cai L, Chen Y, Xue H, et al. Effect and pharmacological mechanism of *Salvia miltiorrhiza* and its characteristic extracts on diabetic nephropathy. *J Ethnopharmacol*. 2024;319(Pt 3):117354. doi:10.1016/j.jep.2023.117354

11. Yang L, Huang X, Wang Z, et al. Research progress on the pharmacological properties of active ingredients from *Salvia miltiorrhiza*: a review. *Phytomedicine*. 2025;148:157272. doi:10.1016/j.phymed.2025.157272
12. Wu Q, Guan YB, Zhang KJ, Li L, Zhou Y. Tanshinone IIA mediates protection from diabetes kidney disease by inhibiting oxidative stress induced pyroptosis. *J Ethnopharmacol*. 2023;316:116667. doi:10.1016/j.jep.2023.116667
13. Cai Y, Zhang W, Chen Z, Shi Z, He C, Chen M. Recent insights into the biological activities and drug delivery systems of tanshinones. *Int J Nanomed*. 2016;11:121–130. doi:10.2147/IJN.S84035
14. Chen F, Li L, Tian DD. *Salvia miltiorrhiza* roots against cardiovascular disease: consideration of herb-drug interactions. *Biomed Res Int*. 2017;2017:9868694. doi:10.1155/2017/9868694
15. Wang F, Feng J, Jin A, et al. Extracellular vesicles for disease treatment. *Int J Nanomed*. 2025;20:3303–3337. doi:10.2147/IJN.S506456
16. Cao M, Diao N, Cai X, et al. Plant exosome nanovesicles (PENs): green delivery platforms. *Mater Horiz*. 2023;10(10):3879–3894. doi:10.1039/d3mh01030a
17. Zou J, Song Q, Shaw PC, Wu Y, Zuo Z, Yu R. Tangerine peel-derived exosome-like nanovesicles alleviate hepatic steatosis induced by type 2 diabetes: evidenced by regulating lipid metabolism and intestinal microflora. *Int J Nanomed*. 2024;19:10023–10043. doi:10.2147/IJN.S478589
18. Fu J, Liu Z, Feng Z, et al. Platycodon grandiflorum exosome-like nanoparticles: the material basis of fresh platycodon grandiflorum optimality and its mechanism in regulating acute lung injury. *J Nanobiotechnol*. 2025;23(1):270. doi:10.1186/s12951-025-03331-z
19. Feng Z, Huang J, Fu J, Li L, Yu R, Li L. Medicinal plant-derived exosome-like nanovesicles as regulatory mediators in microenvironment for disease treatment. *Int J Nanomed*. 2025;20:8451–8479. doi:10.2147/IJN.S526287
20. Liu X, Teng X, Wang J, et al. Exosome-based mucosal therapeutic and diagnostic system: towards clinical translation. *J Control Release*. 2025;385:113966. doi:10.1016/j.jconrel.2025.113966
21. Fang Z, Liu K. Plant-derived extracellular vesicles as oral drug delivery carriers. *J Control Release*. 2022;350:389–400. doi:10.1016/j.jconrel.2022.08.046
22. Guan X, Zhu M, Zhu H, et al. Oral natural extracellular vesicles for biomedical applications: advances and clinical perspectives. *J Adv Res*. 2025. doi:10.1016/j.jare.2025.08.003
23. Huang J, Feng Z, Fu J, et al. Amelioration of acute lung injury by *Salvia miltiorrhiza*-derived extracellular vesicles: through repair of the vascular barrier and modulation of lung microbiota. *Chin Med*. 2026;21(1):6. doi:10.1186/s13020-025-01203-0
24. Shi R, Tan W, Jin H, et al. MicroRNA-enriched plant-derived exosomes alleviate colitis by modulating systemic immunity, metabolic homeostasis, and gut microbiota. *Adv Sci*. 2025;12(42):e05921. doi:10.1002/advs.202505921
25. Dong Y, Tong Y. Lipid peroxidation in diabetic kidney disease: mechanism and natural solution. *Int J Mol Sci*. 2025;26(19):9764. doi:10.3390/ijms26199764
26. Wu Y, Cao Y, Feng L, et al. The natural compound stachyose targets SGLT2-mediated metabolic reprogramming to ameliorate diabetic kidney disease. *Phytomedicine*. 2025;147:157182. doi:10.1016/j.phymed.2025.157182
27. Liu J, Guo M, Yuan X, Fan X, Wang J, Jiao X. Gut microbiota and their metabolites: the hidden driver of diabetic nephropathy? Unveiling gut microbe's role in DN. *J Diabetes*. 2025;17(4):e70068. doi:10.1111/1753-0407.70068
28. Tu QM, Jin HM, Yang XH. Lipid abnormality in diabetic kidney disease and potential treatment advancements. *Front Endocrinol*. 2025;16:1503711. doi:10.3389/fendo.2025.1503711
29. Sen U. Gut microbiota and well-being: a comprehensive summary of the special issue. *Pharmacol Res*. 2025;216:107791. doi:10.1016/j.phrs.2025.107791
30. Huang J, Yu Y, Feng Z, et al. Cross - kingdom dialogue of microbial messengers: multi - target regulatory mechanisms and therapeutic strategies of gut microbiota - derived extracellular vesicles in metabolic diseases. *Int J Nanomed*. 2025;20:12573–12591. doi:10.2147/IJN.S548624
31. Yan K, Sun X, Wang X, Zheng J, Yu H. Gut microbiota and metabolites: biomarkers and therapeutic targets for diabetes mellitus and its complications. *Nutrients*. 2025;17(16):2603. doi:10.3390/nu17162603
32. Zhu Y, Chen B, Zhang X, et al. Exploration of the muribaculaceae family in the gut microbiota: diversity, metabolism, and function. *Nutrients*. 2024;16(16):2660. doi:10.3390/nu16162660
33. Singh SB, Coffman CN, Varga MG, Carroll-Portillo A, Braun CA, Lin HC. Intestinal alkaline phosphatase prevents sulfate reducing bacteria-induced increased tight junction permeability by inhibiting snail pathway. *Front Cell Infect Microbiol*. 2022;12:882498. doi:10.3389/fcimb.2022.882498
34. Sun Y, Chen X, Wang T, et al. Siweixizangmaoru decoction attenuates collagen-induced arthritis via gut microbiota-dependent SCFA restoration and immunomodulation. *Phytomedicine*. 2025;148:157249. doi:10.1016/j.phymed.2025.157249
35. Yu W, Haoyu Y, Ling Z, et al. Targeting lipid metabolic reprogramming to alleviate diabetic kidney disease: molecular insights and therapeutic strategies. *Front Immunol*. 2025;16:1549484. doi:10.3389/fimmu.2025.1549484
36. Zhang Y, Liu Y, Sun J, Zhang W, Guo Z, Ma Q. Arachidonic acid metabolism in health and disease. *MedComm*. 2023;4(5):e363. doi:10.1002/mco2.363
37. Wang YN, Zhang ZH, Liu HJ, et al. Integrative phosphatidylcholine metabolism through phospholipase A2 in rats with chronic kidney disease. *Acta Pharmacol Sin*. 2023;44(2):393–405. doi:10.1038/s41401-022-00947-x
38. Yoshioka K, Hirakawa Y, Kurano M, et al. Lysophosphatidylcholine mediates fast decline in kidney function in diabetic kidney disease. *Kidney Int*. 2022;101(3):510–526. doi:10.1016/j.kint.2021.10.039
39. Zhang Y, Li Y, Quan Z, Xiao P, Duan JA. New insights into antioxidant peptides: an overview of efficient screening, evaluation models, molecular mechanisms, and applications. *Antioxidants*. 2024;13(2):203. doi:10.3390/antiox13020203
40. Hajib A, El Harkaoui S, Choukri H, et al. Apiaceae family an important source of petroselinic fatty acid: abundance, biosynthesis, chemistry, and biological proprieties. *Biomolecules*. 2023;13(11):1675. doi:10.3390/biom13111675
41. Liu L, Xu J, Zhang Z, et al. Metabolic homeostasis of amino acids and diabetic kidney disease. *Nutrients*. 2022;15(1):184. doi:10.3390/nu15010184
42. Peláez R, Pariente A, Pérez-Sala Á, Larráyoz IM. Sterculic acid: the mechanisms of action beyond Stearoyl-CoA Desaturase inhibition and therapeutic opportunities in human diseases. *Cells*. 2020;9(1):140. doi:10.3390/cells9010140
43. Dong Y, Zhang L, Qiu D, et al. Lactobacillus murinus ZNL-13 modulates intestinal barrier damage and gut microbiota in cyclophosphamide-induced immunosuppressed mice. *Foods*. 2025;14(8):1416. doi:10.3390/foods14081416

44. Wang X, Liu X, Gong F, et al. Targeting gut microbiota for diabetic nephropathy treatment: probiotics, dietary interventions, and fecal microbiota transplantation. *Front Endocrinol*. 2025;16:1621968. doi:10.3389/fendo.2025.1621968
45. Noh MR, Jang HS, Salem FE, Ferrer FA, Kim J, Padanilam BJ. Epoxyeicosatrienoic acid administration or soluble epoxide hydrolase inhibition attenuates renal fibrogenesis in obstructive nephropathy. *Am J Physiol Renal Physiol*. 2023;324(2):F138–F151. doi:10.1152/ajprenal.00052.2022